Sensor-based Complementary Globally Asymptotically Stable Filters for Attitude Estimation

Pedro Batista, Carlos Silvestre, Paulo Oliveira

***Abstract*— This paper presents the design, analysis, and performance evaluation of globally asymptotically stable filters for attitude estimation. The design is based directly on the sensor measurements as opposed to traditional solutions that resort to parameterizations of the rotation, e.g., Euler angles or quaternions, or more recent geometric approaches explicitly solved on the special orthogonal group, $SO(3)$. The proposed solutions include the estimation of gyro bias, incomplete sensor measurements, systematic tuning procedures, and also allow for the inclusion of frequency weights to model colored noise. Finally, and due to the inherent structure, the filters are complementary and also cope well with slowly time-varying gyro bias. Simulation results are included that illustrate the achievable performance in the presence of realistic measurements provided by low-cost, low-power sensor suites.**

I. Introduction

The design of Navigation Systems plays a key role in the development of a large variety of mobile platforms. Indeed, the quality of the navigation information is a fundamental requirement in many applications, whether it is for data acquisition purposes, where geo-referencing is usually essential, or for control purposes, where quantities such as the position, attitude, and the linear and angular velocities of the vehicle are often required. This paper presents the analysis, design, and performance evaluation of globally asymptotically stable filter for attitude estimation based directly on the sensor measurements.

Traditional attitude estimation methods consist, as discussed in the recent survey paper [1], in a two step process: i) estimate the attitude from body measurements and known reference observations, and ii) filtering the noisy quantities. The first step, where an attitude estimate is obtained from body measurements to feed a filter (or an observer), ends up in one of many known representations, e.g., Euler angles, quaternions, Euler angle-axis representation, rotation matrix, etc. [2]. The filtering process builds essentially on a kinematic model combined either with the integration of rate-gyros or dynamic models. In the first case, the kinematics are propagated using three-axis rate gyros, while in the second case the dynamic model for the angular velocity is used. Each has its own advantages and disadvantages. For instance, dynamic models are complex, highly nonlinear, often time-varying, and the inertia matrix may not be well known, as well as other dynamic parameters. On the other hand, rate-gyros are usually subject to measurement bias, often slowly time-varying. With all possible combinations, attitude estimation solutions are many in the literature. Extended Kalman Filters (EKFs) and variants have been widely used, see [3] and [4], for instance. In spite of the good performance achieved by EKF and EKF-like solutions, divergence due to the linearization of the system dynamics has led to the pursuit of different solutions, in particular nonlinear observers such as those presented in [5] and [6]. For a more thorough survey, the reader is referred to [1]. In all the aforementioned references, the sensor measurements are essentially used to obtain instantaneous algebraic measurements of the attitude that are used afterwards to feed an observer or filter, depending on whether or not sensor noise is considered. Sensor specificness is therefore disregarded and, even when it is considered, the nonlinear transformations that are performed to obtain the attitude from vector measurements distort noise characteristics. Moreover, with the exception of EKF and EKF-like solutions, systematic tuning procedures are often absent. Exceptions are presented in [7] and [8] where vector measurements are used directly in the feedback of observers built directly on the Special Orthogonal Group $SO(3)$ and the Special Euclidean Group $SE(3)$, respectively. In the first local exponential stability is achieved and the error is shown to converge to zero for almost all initial conditions, while in the second case almost global exponential stability (AGES) is achieved for the observer error dynamics.

The main contribution of this paper is the development of sensor-based attitude estimation filter solutions that

- are based on the exact angular motion kinematics;
- build on the well-established Kalman filtering theory;
- have globally asymptotically stable (GAS) error dynamics;
- provide systematic tuning procedures based directly on the sensor specifications, including also frequency weights in the design to model colored noise;
- estimate rate gyro bias and cope well with slowly time-varying bias; and
- have a complementary structure, fusing low bandwidth vector observations with high bandwidth rate gyro measurements.

As previously mentioned, traditional attitude solutions use the sensor measurements to obtain instantaneous attitude measurements and the filter process resorts to one of many attitude representation alternatives. In this paper the sensor measurements are included directly in the system dynamics and the kinematics are propagated using the angular velocity provided by a three-axis rate gyro, whose bias is also considered. In addition to that, the case of insufficient vector measurement observations for attitude estimation is also addressed. Essential in the observability analysis and filter design is the modification of the system dynamics to yield a structure that can be regarded as linear time-

The work of P. Batista was supported by a PhD Student Scholarship from the POCTI Programme of FCT, SFRH/BD/24862/2005.

The authors are with the Institute for Systems and Robotics, Instituto Superior Técnico, Av. Rovisco Pais, 1049-001 Lisboa, Portugal. {pbatista,cjs,pjcro}@isr.ist.utl.pt

varying (LTV), although it is, in fact, nonlinear. However, the system dynamics are still exact and no linearization is performed whatsoever. Observability analysis follows, for single and double vector observations, and then the Kalman filter design, whose stability is well characterized given the observability properties that are derived in the paper. The final attitude estimation solution results from combining the sensor-based filter with an optimal attitude determination algorithm. This last problem is commonly known in the literature as the Wahba's problem [9] and, for two vector observations, there are closed-form solutions, see [10], [11], [1], and references therein.

The paper is organized as follows. The sensor-based frameworks that are the core of the proposed solutions are presented in Section II, and, in Section III, the observability properties of the systems are derived. The filtering design is addressed in Section IV and the achieved performance evaluated in Section V in realistic simulation environments. Finally, Section VI summarizes the main contributions and conclusions of the paper.

A. Notation

Throughout the paper the symbol $\mathbf{0}$ denotes a matrix (or vector) of zeros and $\mathbf{I}$ an identity matrix, both of appropriate dimensions. A block diagonal matrix is represented as $\mathrm{diag}(\mathbf{A}_1, \ldots, \mathbf{A}_\mathrm{n})$. If $\mathbf{x}$ and $\mathbf{y}$ are two vectors of identical dimensions, $\mathbf{x} \times \mathbf{y}$ and $\mathbf{x} \cdot \mathbf{y}$ are the cross and inner products, respectively.

II. Sensor-based Framework

A. System dynamics

Let $\{I\}$ denote a local inertial frame, $\{B\}$ the body-fixed frame, and $\mathbf{R}$ the rotation matrix from $\{B\}$ to $\{I\}$. The attitude kinematics may be described, using this representation in $SO(3)$, as

$$\dot{\mathbf{R}}(t) = \mathbf{R}(t)\mathbf{S}\left[\boldsymbol{\omega}(t)\right],$$

where $\boldsymbol{\omega} \in \mathbb{R}^3$ is the angular velocity of $\{B\}$, expressed in $\{B\}$, and $\mathbf{S}(\boldsymbol{x})$ is the skew-symmetric matrix such that $\mathbf{S}(\boldsymbol{x})\,\boldsymbol{y} = \boldsymbol{x} \times \boldsymbol{y}$. For the sake of generality, suppose that measurements $\mathbf{y}_1 \in \mathbb{R}^3$ and $\mathbf{y}_2 \in \mathbb{R}^3$ are available, in body-fixed coordinates, of known constant quantities in inertial coordinates,

$$^I\mathbf{y}_1 = \mathbf{R}(t)\mathbf{y}_1(t)$$

and

$$^I\mathbf{y}_2 = \mathbf{R}(t)\mathbf{y}_2(t),$$

respectively. Then, the dynamics of $\mathbf{y}_1$ and $\mathbf{y}_2$ are given by

$$\begin{cases} \dot{\mathbf{y}}_1 = -\mathbf{S}\left[\boldsymbol{\omega}(t)\right]\mathbf{y}_1 \\ \dot{\mathbf{y}}_2 = -\mathbf{S}\left[\boldsymbol{\omega}(t)\right]\mathbf{y}_2 \end{cases}.$$

Further consider rate-gyro measurements $\boldsymbol{\omega}_m \in \mathbb{R}^3$ corrupted with bias $\mathbf{b}_{\boldsymbol{\omega}} \in \mathbb{R}^3$, i.e.,

$$\boldsymbol{\omega}_m(t) = \boldsymbol{\omega}(t) + \mathbf{b}_{\boldsymbol{\omega}}(t).$$

Then, for double vector observations the system dynamics may be written as

$$\begin{cases} \dot{\mathbf{x}}_1(t) = -\mathbf{S}\left[\boldsymbol{\omega}_m(t)\right]\mathbf{x}_1(t) + \mathbf{S}\left[\mathbf{b}_{\boldsymbol{\omega}}(t)\right]\mathbf{x}_1(t) \\ \dot{\mathbf{x}}_2(t) = -\mathbf{S}\left[\boldsymbol{\omega}_m(t)\right]\mathbf{x}_2(t) + \mathbf{S}\left[\mathbf{b}_{\boldsymbol{\omega}}(t)\right]\mathbf{x}_2(t) \\ \dot{\mathbf{b}}_{\boldsymbol{\omega}}(t) = \mathbf{0} \\ \mathbf{y}_1(t) = \mathbf{x}_1(t) \\ \mathbf{y}_2(t) = \mathbf{x}_2(t) \end{cases} \quad (1)$$

and, for single vector observations, as

$$\begin{cases} \dot{\mathbf{x}}_r(t) = -\mathbf{S}\left[\boldsymbol{\omega}_m(t)\right]\mathbf{x}_r(t) + \mathbf{S}\left[\mathbf{b}_{\boldsymbol{\omega}}(t)\right]\mathbf{x}_r(t) \\ \dot{\mathbf{b}}_{\boldsymbol{\omega}}(t) = \mathbf{0} \\ \mathbf{y}_r(t) = \mathbf{x}_r(t) \end{cases}, \quad (2)$$

where $\mathbf{x}_r$ and $\mathbf{y}_r$ are used instead of $\mathbf{x}_1$ and $\mathbf{y}_1$ as there is only one vector measurement. The problem considered in the paper is the design of filter solutions for the nonlinear systems (1) and (2). Notice that, once filtered estimates of $\mathbf{x}_1$ and $\mathbf{x}_2$ are obtained, the attitude is immediately obtained as in tradition methods.

B. Practical considerations

Many vector observations may be considered. Common Inertial Measurement Units (IMU) contain three triads of orthogonally-mounted rate-gyros, accelerometers, and magnetometers. The magnetometers provide the magnetic field in body-fixed coordinates. This quantity is locally constant in inertial coordinates and it is therefore on feasible vector observation, as discussed in [7]. On the other hand, for sufficiently low frequency bandwidths, the gravitational field also dominates the accelerometer measurement, as discussed in [7]. Therefore, this would provide a second vector observation, but there are other alternatives. For example, in [8] a set of known landmarks is assumed to be fixed in the inertial frame and their position with respect to $\{B\}$ is measured, in body-fixed coordinates. The difference between any pair of landmark readings also consists in a valid vector observation. Other possibilities include vision systems, sonar readings, radar readings, star trackers, etc. Finally, notice that, if the attitude is single-handed for filtering processes, without any vector observations, any pair of columns of the rotation matrix $\mathbf{R}(t)$ can also be regarded as two vector observations.

It is well known that, for two nonparallel vector observations, the attitude is uniquely determined, and for a single vector observation, it is impossible to determine the attitude. However, there is still some interest in the study of this case. Dead-reckoning navigation systems such as Inertial Navigation Systems (INS) provide open-loop propagation of the motion state. However, the estimation of the position and attitude of the vehicle is necessarily obtained in this type of systems by integrating higher-order derivatives such as the linear acceleration and the angular velocity. As such, and regardless of the accuracy and precision of the IMU, the errors in the position and attitude estimates grow unbounded due to the noise and bias of the sensors [12]. A single vector observation does not provide the entire attitude but it may help compensating bias and restricting the attitude to a set of lower dimensions. For example, a gravitation field measurement yields the roll and pitch Euler angles of a yaw, pitch, and roll Euler angles representation.

Finally, it is important to remark that, although only two vector observations are considered, more may be incorporated in the filter design. The analysis of observability does not change for more than two nonparallel vector observations and the system dynamics are trivially extended.

III. Observability analysis

A. Uniform complete observability

Consider the LTV system

$$\left\{ \begin{array}{l} \dot{\mathbf{x}}(t) = \mathbf{A}(t)\mathbf{x}(t) + \mathbf{B}(t)\mathbf{u}(t) \\ \mathbf{y}(t) = \mathbf{C}(t)\mathbf{x}(t) \end{array} \right. , \tag{3}$$

where $\mathbf{x}$, $\mathbf{u}$, $\mathbf{y}$ are the state, input, and output of the system, respectively, $t \in [t_0, +\infty[$, and $\mathbf{A}(t)$, $\mathbf{B}(t)$, and $\mathbf{C}(t)$ are continuous matrices of compatible dimensions.

Definition 3.1 (Uniform complete observability): The LTV system (3) is called *uniformly completely observable* if there exist positive constants δ, α_1, and α_2 such that

$$\alpha_1 \mathbf{I} \preceq \boldsymbol{\mathcal{W}}(t, t+\delta) \preceq \alpha_2 \mathbf{I} \tag{4}$$

for all $t \geq t_0$, where $\boldsymbol{\mathcal{W}}(t_0, t_f)$ is the observability Gramian associated with the pair $(\mathbf{A}(t), \mathbf{C}(t))$.

Remark 1: When the system matrices $\mathbf{A}(t)$ and $\mathbf{C}(t)$ are norm-bounded, it is easy to see that the right side of (3) is always satisfied. This is the case of the systems under study in the paper and therefore only the left side of (4) is considered and the existence of α_2 needs not to be addressed.

B. Double vector observations

The observability of (1) is examined in this section. The states $\mathbf{x}_1$ and $\mathbf{x}_2$ are obviously observable as they are measured. Therefore the question is to determine the conditions such that it is possible to determine the rate gyro bias. These conditions are well known but, for stability purposes, stronger results are convenient, e.g., uniform complete observability. On the other hand, the system dynamics (1) are nonlinear. Notice, however, that using the cross product properties $\boldsymbol{x} \times \boldsymbol{y} = -\boldsymbol{y} \times \boldsymbol{x}$, it is possible to rewrite(1) as

$$\left\{ \begin{array}{l} \dot{\mathbf{x}}_1(t) = -\mathbf{S}\left[\boldsymbol{\omega}_m(t)\right]\mathbf{x}_1(t) - \mathbf{S}\left[\mathbf{x}_1(t)\right]\mathbf{b}_{\boldsymbol{\omega}}(t) \\ \dot{\mathbf{x}}_2(t) = -\mathbf{S}\left[\boldsymbol{\omega}_m(t)\right]\mathbf{x}_2(t) - \mathbf{S}\left[\mathbf{x}_2(t)\right]\mathbf{b}_{\boldsymbol{\omega}}(t) \\ \dot{\mathbf{b}}_{\boldsymbol{\omega}}(t) = \mathbf{0} \\ \mathbf{y}_1(t) = \mathbf{x}_1(t) \\ \mathbf{y}_2(t) = \mathbf{x}_2(t) \end{array} \right.$$

or, in compact form, as

$$\left\{ \begin{array}{l} \dot{\boldsymbol{x}}(t) = \mathbf{A}(t)\boldsymbol{x}(t) \\ \mathbf{y}(t) = \mathbf{C}\boldsymbol{x}(t) \end{array} \right. , \tag{5}$$

where

$$\mathbf{A}(t) = \left[\begin{array}{ccc} -\mathbf{S}\left[\boldsymbol{\omega}_m(t)\right] & \mathbf{0} & -\mathbf{S}\left[\mathbf{y}_1(t)\right] \\ \mathbf{0} & -\mathbf{S}\left[\boldsymbol{\omega}_m(t)\right] & -\mathbf{S}\left[\mathbf{y}_2(t)\right] \\ \mathbf{0} & \mathbf{0} & \mathbf{0} \end{array} \right]$$

and

$$\mathbf{C} = \left[\begin{array}{cc} \mathbf{I} & \mathbf{0} \\ \mathbf{0} & \mathbf{I} \end{array} \right].$$

Now, although the system dynamics (5) are nonlinear, they may, nevertheless, be regarded as LTV. This allows for the derivation of important observability results and the design of a GAS Kalman filter. Before addressing the first of these issues, the following lemma is introduced.

Lemma 1: Let $\mathbf{f}(t) : [t_0, t_f] \subset \mathbb{R} \rightarrow \mathbb{R}^n$ be a continuous and two times continuously differentiable function on $\mathcal{I} := [t_0, t_f]$, $T := t_f - t_0 > 0$, and such that

$$\mathbf{f}(t_0) = \mathbf{0}.$$

Further assume that

$$\max_{t \in \mathcal{I}} \left\| \ddot{\mathbf{f}}(t) \right\| \leq C. \tag{6}$$

If

$$\begin{array}{c} \exists \quad : \quad \left\| \dot{\mathbf{f}}(t^*) \right\| \geq \alpha^*, \\ \alpha^* > 0 \\ t^* \in \mathcal{I} \end{array} \tag{7}$$

then

$$\begin{array}{c} \exists \quad : \quad \left\| \mathbf{f}(t_0 + \delta^*) \right\| \geq \beta^*. \\ 0 < \delta^* \leq T \\ \beta^* > 0 \end{array} \tag{8}$$

The following theorem addresses the observability of (5).

Theorem 1: The LTV system (5) is uniformly completely observable if and only if the vector observations are not parallel or, equivalently,

$${}^{I}\mathbf{y}_1 \times {}^{I}\mathbf{y}_2 \neq \mathbf{0}. \tag{9}$$

Proof: Let $\mathbf{R}_m(t) \in SO(3)$ be a rotation matrix such that

$$\dot{\mathbf{R}}_m(t) = \mathbf{R}_m(t)\mathbf{S}\left[\boldsymbol{\omega}_m(t)\right]$$

and consider the Lyapunov transformation [13]

$$\mathbf{z}(t) = \mathbf{T}(t)\boldsymbol{x}(t),$$

which preserves observability properties, where

$$\mathbf{T}(t) = \mathrm{diag}\left(\mathbf{R}_{\mathrm{m}}(t), \mathbf{R}_{\mathrm{m}}(t), \mathbf{I}\right).$$

It is a simple matter of computation to show that the new system dynamics are given by

$$\left\{ \begin{array}{l} \dot{\mathbf{z}}(t) = \boldsymbol{\mathcal{A}}(t)\mathbf{z}(t) \\ \mathbf{y}(t) = \boldsymbol{\mathcal{C}}(t)\mathbf{z}(t) \end{array} \right. ,$$

where

$$\boldsymbol{\mathcal{A}}(t) = \left[\begin{array}{ccc} \mathbf{0} & \mathbf{0} & -\mathbf{R}_m(t)\mathbf{S}\left[\mathbf{y}_1(t)\right] \\ \mathbf{0} & \mathbf{0} & -\mathbf{R}_m(t)\mathbf{S}\left[\mathbf{y}_2(t)\right] \\ \mathbf{0} & \mathbf{0} & \mathbf{0} \end{array} \right]$$

and

$$\boldsymbol{\mathcal{C}}(t) = \left[\begin{array}{cc} \mathbf{R}_m^T(t) & \mathbf{0} \\ \mathbf{0} & \mathbf{R}_m^T(t) \end{array} \right].$$

The transition matrix associated with $\boldsymbol{\mathcal{A}}(t)$ is given by

$$\boldsymbol{\phi}(t, t_0) = \left[\begin{array}{ccc} \mathbf{I} & \mathbf{0} & -\int_{t_0}^{t} \mathbf{R}_m(\sigma)\mathbf{S}\left[\mathbf{y}_1(\sigma)\right] d\sigma \\ \mathbf{0} & \mathbf{I} & -\int_{t_0}^{t} \mathbf{R}_m(\sigma)\mathbf{S}\left[\mathbf{y}_2(\sigma)\right] d\sigma \\ \mathbf{0} & \mathbf{0} & \mathbf{I} \end{array} \right]$$

and, if $\boldsymbol{\mathcal{W}}(t_0, t_f)$ denotes the observability Gramian associated with the pair $(\boldsymbol{\mathcal{A}}(t), \boldsymbol{\mathcal{C}}(t))$ on $[t_0, t_f]$ and $\mathbf{d} = \left[\mathbf{d}_1^T \ \mathbf{d}_2^T \ \mathbf{d}_3^T\right]^T$, $\|\mathbf{d}\| = 1$, it is a simple matter of computation to show that

$$\mathbf{d}^T \boldsymbol{\mathcal{W}}(t, t+\delta)\, \mathbf{d} = \int_t^{t+\delta} \left\| \mathbf{f}(\tau) \right\|^2 d\tau,$$

where

$$\mathbf{f}(\tau) := \left[\begin{array}{c} \mathbf{d}_1 - \int_t^{\tau} \mathbf{R}_m(\sigma)\mathbf{S}\left[\mathbf{y}_1(\sigma)\right]\mathbf{d}_3 d\sigma \\ \mathbf{d}_2 - \int_t^{\tau} \mathbf{R}_m(\sigma)\mathbf{S}\left[\mathbf{y}_2(\sigma)\right]\mathbf{d}_3 d\sigma \end{array} \right].$$

For $\mathbf{d}_1 \neq \mathbf{0}$ or $\mathbf{d}_2 \neq \mathbf{0}$ it is clear that $\|\mathbf{f}(0)\| \geq \|\mathbf{d}_1\| = \alpha_1^*$ or $\|\mathbf{f}(0)\| \geq \|\mathbf{d}_2\| = \alpha_2^*$, respectively. On the other hand, if $\mathbf{d}_1 = \mathbf{d}_2 = \mathbf{0}$, it follows that $\|\mathbf{d}_3\| = 1$,

$$\mathbf{f}(t) = \mathbf{0},$$

and

$$\dot{\mathbf{f}}(t) = -\begin{bmatrix} \mathbf{R}_m(t)\mathbf{S}[\mathbf{y}_1(t)]\,\mathbf{d}_3 \\ \mathbf{R}_m(t)\mathbf{S}[\mathbf{y}_2(t)]\,\mathbf{d}_3 \end{bmatrix}.$$

Now, suppose that (9) is true. Then,

$$\mathbf{y}_1(t) \times \mathbf{y}_2(t) \neq \mathbf{0}$$

for all $t \geq t_0$. Therefore, there exists $\alpha_3^* > 0$ such that

$$\left\|\dot{\mathbf{f}}(t)\right\| \geq \alpha_3^*$$

for all $t \geq t_0$ and $\|\mathbf{d}_3\| = 1$. But that means, using Lemma 1, that there exist $\alpha_4^* > 0$ and $\delta_1^* > 0$ such that

$$\|\mathbf{f}(t + \delta_1^*)\| \geq \alpha_4^*$$

for all $t \geq t_0$. Therefore

$$\begin{array}{ccccc} \exists & & \forall & \forall & : \\ \alpha^* > 0 & & t \geq t_0 & \mathbf{d} \in \mathbb{R}^9 & \\ \delta^* > 0 & & & \|\mathbf{d}\| = 1 & \end{array} \quad \|\mathbf{f}(t + \delta^*)\| \geq \alpha^*,$$

and using Lemma 1 again,

$$\begin{array}{ccccc} \exists & & \forall & \forall & : \\ \alpha > 0 & & t \geq t_0 & \mathbf{d} \in \mathbb{R}^9 & \\ \delta > 0 & & & \|\mathbf{d}\| = 1 & \end{array} \quad \mathbf{d}^T \boldsymbol{\mathcal{W}}(t, t + \delta)\,\mathbf{d} \geq \alpha,$$

which means that the system is uniformly completely observable. Suppose now that (9) is not true. Then,

$$\mathbf{y}_1(t) \times \mathbf{y}_2(t) = \mathbf{0}$$

for all $t \geq t_0$ and

$$\begin{array}{ccccc} \exists & & \forall & : & \\ \mathbf{d}_3 \in \mathbb{R}^3 & & t \geq t_0 & & \\ \|\mathbf{d}_3\| = 1 & & & & \end{array} \quad \mathbf{y}_1(t) \times \mathbf{d}_3 = \mathbf{y}_2(t) \times \mathbf{d}_3 = \mathbf{0}.$$

Let

$$\mathbf{d} = \begin{bmatrix} \mathbf{0} \\ \mathbf{0} \\ \mathbf{d}_3 \end{bmatrix}.$$

It is straightforward to show that

$$\mathbf{d}^T \boldsymbol{\mathcal{W}}(t, t + \delta)\,\mathbf{d} = 0$$

for all $t \geq t_0$. Therefore, the system is not observable, which concludes the proof, as in that case it is not uniformly completely observable either. ■

This result, although quite simple, is nevertheless fundamental to assess about the stability of the Kalman filter that will be presented in Section IV.

C. Single vector observations

As it was previously mentioned, with a single vector measurement it is impossible to determine the attitude uniquely. However, it may still be possible to restrict the attitude to a space of lower dimension and determine the gyro bias. Before providing the main result, notice that, as in the previous case, the nonlinear system (2) may be rewritten, in a compact form, as

$$\begin{cases} \dot{\boldsymbol{x}}_r(t) = \mathbf{A}_r(t)\boldsymbol{x}_r(t) \\ \mathbf{y}_r(t) = \mathbf{C}_r\boldsymbol{x}_r(t) \end{cases}, \tag{10}$$

where

$$\mathbf{A}_r(t) = \begin{bmatrix} -\mathbf{S}[\boldsymbol{\omega}_m(t)] & -\mathbf{S}[\mathbf{y}_r(t)] \\ \mathbf{0} & \mathbf{0} \end{bmatrix}$$

and

$$\mathbf{C}_r = \begin{bmatrix} \mathbf{I} & \mathbf{0} \end{bmatrix},$$

which may be regarded as a LTV system, although it is in fact nonlinear. The following theorem provides a necessary and sufficient condition on uniform complete observability for (10).

Theorem 2: The LTV system (10) is uniformly completely observable if and only if

$$\begin{array}{ccccc} \exists & \forall & \forall & \exists & : \\ \delta^* > 0 & t \geq t_0 & \mathbf{d} \in \mathbb{R}^3 & t^* \in [t, t + \delta^*] & \\ \alpha^* > 0 & & \|\mathbf{d}\| = 1 & & \end{array} \quad \|\mathbf{S}(\mathbf{y}_r(t^*))\,\mathbf{d}\| \geq \alpha^*. \tag{11}$$

Proof: Following the same steps as in Theorem 1, consider the Lyapunov transformation

$$\mathbf{z}_r(t) = \mathbf{T}_r(t)\boldsymbol{x}_r(t),$$

which preserves observability properties, where

$$\mathbf{T}_r(t) = \mathrm{diag}\left(\mathbf{R}_{\mathrm{m}}(\mathrm{t}),\, \mathbf{I}\right).$$

It is a simple matter of computation to show that the new system dynamics are given by

$$\begin{cases} \dot{\mathbf{z}}_r(t) = \boldsymbol{\mathcal{A}}_r(t)\mathbf{z}_r(t) \\ \mathbf{y}_r(t) = \boldsymbol{\mathcal{C}}_r(t)\mathbf{z}_r(t) \end{cases},$$

where

$$A_z(t) = \begin{bmatrix} \mathbf{0} & -\mathbf{R}_m(t)\mathbf{S}[\mathbf{y}_r(t)] \\ \mathbf{0} & \mathbf{0} \end{bmatrix}$$

and

$$C_z(t) = \begin{bmatrix} \mathbf{R}_m^T(t) & \mathbf{0} \end{bmatrix}.$$

The transition matrix associated with $\boldsymbol{\mathcal{A}}_r(t)$ is given by

$$\boldsymbol{\phi}(t, t_0) = \begin{bmatrix} \mathbf{I} & -\int_{t_0}^{t} \mathbf{R}_m(\sigma)\mathbf{S}[\mathbf{y}_r(\sigma)]\,d\sigma \\ \mathbf{0} & \mathbf{I} \end{bmatrix}$$

and, if $\boldsymbol{\mathcal{W}}_r(t_0, t_f)$ denotes the observability Gramian associated with the pair $(\boldsymbol{\mathcal{A}}_r(t), \boldsymbol{\mathcal{C}}_r(t))$ on $[t_0, t_f]$ and $\mathbf{d} = \begin{bmatrix} \mathbf{d}_1^T & \mathbf{d}_2^T & \mathbf{d}_3^T \end{bmatrix}^T$, $\|\mathbf{d}\| = 1$, it is a simple matter of computation to show that

$$\mathbf{d}^T \boldsymbol{\mathcal{W}}_r(t, t + \delta)\,\mathbf{d} = \int_t^{t+\delta} \|\mathbf{f}_r(\tau)\|^2 d\tau,$$

where

$$\mathbf{f}_r(\tau) := \mathbf{d}_1 - \int_t^{\tau} \mathbf{R}_m(\sigma)\mathbf{S}[\mathbf{y}_r(\sigma)]\,\mathbf{d}_2 d\sigma.$$

Suppose now that (11) is true. Notice that, if $\mathbf{d}_1 \neq \mathbf{0}$, there exists $\alpha_1^* > 0$

$$\|\mathbf{f}_r(t)\| = \alpha_1^*$$

for all $t \geq t_0$. On the other hand, if $\mathbf{d}_1 = \mathbf{0}$, it is straightforward to show, using (11), that

$$\begin{array}{cccc} \exists & \forall & \forall & \exists \\ \delta_2^* > 0 & t \geq t_0 & \mathbf{d}_2 \in \mathbb{R}^3 & t_2^* \in [t, t+\delta_2^*] \\ \alpha_2^* > 0 & & \|\mathbf{d}_2\| = 1 & \end{array} : \left\| \dot{\mathbf{f}}_r\left(t_2^*\right) \right\| \geq \alpha_2^*.$$

In addition to that, notice that $\ddot{\mathbf{f}}_r(\tau)$ is bounded for all τ and $\mathbf{f}_r(t) = \mathbf{0}$. Therefore, resorting to Lemma 1, it follows that

$$\begin{array}{cccc} \exists & \forall & \forall & \exists \\ \delta_3^* > 0 & t \geq t_0 & \mathbf{d}_2 \in \mathbb{R}^3 & t_3^* \in [t, t+\delta_3^*] \\ \alpha_3^* > 0 & & \|\mathbf{d}_2\| = 1 & \end{array} : \|\mathbf{f}_r\left(t_3^*\right)\| \geq \alpha_3^*.$$

But then it is possible to write

$$\begin{array}{cccc} \exists & \forall & \forall & \exists \\ \delta_4^* > 0 & t \geq t_0 & \mathbf{d} \in \mathbb{R}^6 & t_4^* \in [t, t+\delta_4^*] \\ \alpha_4^* > 0 & & \|\mathbf{d}\| = 1 & \end{array} : \|\mathbf{f}_r\left(t_4^*\right)\| \geq \alpha_4^*$$

and, using Lemma 1 again, it follows that

$$\begin{array}{cccc} \exists & \forall & \forall & \exists \\ \delta^* > 0 & t \geq t_0 & \mathbf{d} \in \mathbb{R}^6 & t^* \in [t, t+\delta^*] \\ \alpha^* > 0 & & \|\mathbf{d}\| = 1 & \end{array} : \mathbf{d}^T \boldsymbol{\mathcal{W}}_r(t, t+\delta)\mathbf{d} \geq \alpha^*,$$

which means that (10) is uniformly completely observable. Next, it is shown that (11) is also a necessary condition. Suppose that (11) is not true. Then,

$$\begin{array}{cccc} \forall & \exists & \exists & \forall \\ \delta > 0 & t^* \geq t_0 & \mathbf{d}^* \in \mathbb{R}^3 & t \in [t^*, t^*+\delta] \\ \alpha > 0 & & \|\mathbf{d}^*\| = 1 & \end{array} : \|\mathbf{S}\left(\mathbf{y}_r\left(t\right)\right)\mathbf{d}^*\| < \alpha. \tag{12}$$

Let

$$\mathbf{d} = \begin{bmatrix} \mathbf{0} \\ \mathbf{d}^* \end{bmatrix}.$$

Then, it is straightforward to conclude that

$$\begin{aligned} \mathbf{d}^T \boldsymbol{\mathcal{W}}_r(t^*, t^*+\delta)\mathbf{d} &= \int_{t_*}^{t^*+\delta} \|\mathbf{f}_r\left(\tau\right)\|^2 d\tau \\ &= \int_{t_*}^{t^*+\delta} \left\| \int_{t^*}^{\tau} \mathbf{R}_m(\sigma)\mathbf{S}\left[\mathbf{y}_r(\sigma)\right]\mathbf{d}^* d\sigma \right\|^2 d\tau \\ &\leq \int_{t_*}^{t^*+\delta} \int_{t^*}^{\tau} \left\|\mathbf{R}_m(\sigma)\mathbf{S}\left[\mathbf{y}_r(\sigma)\right]\mathbf{d}^*\right\|^2 d\sigma d\tau \\ &= \int_{t_*}^{t^*+\delta} \int_{t^*}^{\tau} \left\|\mathbf{S}\left[\mathbf{y}_r(\sigma)\right]\mathbf{d}^*\right\|^2 d\sigma d\tau \\ &= \left\|\mathbf{S}\left(\mathbf{y}_r\left[\xi(\delta)\right]\right)\mathbf{d}^*\right\|^2 \int_{t_*}^{t^*+\delta} \int_{t^*}^{\tau} 1 d\sigma d\tau \\ &= \left\|\mathbf{S}\left(\mathbf{y}_r\left[\xi(\delta)\right]\right)\mathbf{d}^*\right\|^2 \tfrac{\delta^2}{2}, \end{aligned} \tag{13}$$

where $\xi(\delta) \in]t^*, t^*+\delta[$. From (12) and (13) it follows that

$$\mathbf{d}^T \boldsymbol{\mathcal{W}}_r(t^*, t^*+\delta)\mathbf{d} \leq \frac{\delta^2}{2}\alpha$$

for all $\alpha > 0$, $\delta > 0$. Let

$$\alpha = \frac{2}{\delta^2}\epsilon.$$

Then,

$$\begin{array}{cccc} \forall & \exists & \exists & \\ \delta > 0 & t^* \geq t_0 & \mathbf{d}^* \in \mathbb{R}^6 & \\ \epsilon > 0 & & \|\mathbf{d}^*\| = 1 & \end{array} : \mathbf{d}^T \boldsymbol{\mathcal{W}}_r(t^*, t^*+\delta)\mathbf{d} < \alpha,$$

which means that the LTV system (10) is not uniformly completely observable. Therefore, if (10) is uniformly completely observable, (11) must hold, which concludes the proof. ■

Remark 2: Technically, (11) may be interpreted as a persistent excitation condition. From the practical point of view, Theorem 2 simply states that the LTV system is uniformly completely observable if and only if there exists $\delta^* > 0$ such that there is a minimal angular motion on any time interval of length δ^*.

IV. Attitude estimation solution

This section presents the attitude estimation solution proposed in the paper. The final structure results from combining a sensor-based globally asymptotically stable Kalman filter, whose design is detailed in Section IV-A, with an optimal and computationally efficient attitude determination algorithm from two vector observations, briefly described in Section IV-B. For single vector observations it is well known that it is impossible to reconstruct the attitude. However, it is still possible to determine, e.g., two Euler angles. This is the last step of the resulting structure for single vector measurements, which is addressed in Section IV-C. Additionally, the problem of more than two vector observations is also briefly discussed, in Section IV-D, and it is shown how easy it is to generalize the previous solution for this case.

A. Filter design

For filtering design purposes, consider an augmented version of (5), given by

$$\begin{cases} \dot{\boldsymbol{x}}(t) = \mathbf{A}(t)\boldsymbol{x}(t) + \mathbf{B}\mathbf{d}(t) \\ \mathbf{y}(t) = \mathbf{C}\boldsymbol{x}(t) + \mathbf{D}\mathbf{n}(t) \end{cases}, \tag{14}$$

where $\mathbf{d}(t)$ and $\mathbf{n}(t)$ are system disturbances and sensor noise, respectively. To model colored noise, it may be assumed that $\mathbf{d}(t)$ and $\mathbf{n}(t)$ are the outputs of stable linear time invariant (LTI) filters $\mathcal{W}_d$ and $\mathcal{W}_n$, respectively, driven by unit intensity continuous-time white Gaussian noise. This assumption leads to an augmented version of the Kalman filter, see [14] for an example of application. In this paper, and for the sake of clarity of presentation, the simple version given by (14) is employed, where $\mathbf{d}$ and $\mathbf{n}$ are assumed zero-mean, white Gaussian noises, with intensity matrices $\boldsymbol{\Xi}$ and $\boldsymbol{\Theta}$, respectively, and correlation matrix $\boldsymbol{\Psi}$. The Kalman filter synthesis is trivial (and therefore omitted) and global asymptotic stability achieved provided that $\mathbf{B}$ and $\mathbf{D}$ are properly chosen, as the pair $(\mathbf{A}(t), \mathbf{C})$ was shown to be uniformly completely observable [15], [16].

B. Attitude determination

The problem of finding the proper rotation matrix $\mathbf{R}$ that minimizes the loss function

$$J\left(\mathbf{R}\right) = \frac{1}{2}\sum_{i=1}^{N} a_i \left\|\mathbf{y}_i - \mathbf{R}^{TI}\mathbf{y}_i\right\|^2,\ a_i > 0,$$

is known in the literature as the Wahba's problem [9] and, for $N = 2$, there exists a closed-loop solution. In the previous section a Kalman filter was derived that yields filtered estimates $\hat{\mathbf{y}}_1(t)$ and $\hat{\mathbf{y}}_2(t)$ of the vector observations $\mathbf{y}_1(t)$ and $\mathbf{y}_2(t)$ provided by the sensors. Instead of using the sensor measurements, the filtered estimates are normalized,

$$\hat{\mathbf{y}}_1^n(t) = \frac{\hat{\mathbf{y}}_1(t)}{\|\hat{\mathbf{y}}_1(t)\|},\ \hat{\mathbf{y}}_2^n(t) = \frac{\hat{\mathbf{y}}_2(t)}{\|\hat{\mathbf{y}}_2(t)\|},$$

as well as the corresponding inertial vectors,

$$ {}^{I}\mathbf{y}_1^u = \frac{{}^{I}\mathbf{y}_1}{\|{}^{I}\mathbf{y}_1\|}, \; {}^{I}\mathbf{y}_2^u = \frac{{}^{I}\mathbf{y}_2}{\|{}^{I}\mathbf{y}_2\|}, $$

and the attitude matrix is reconstructed using the closed-loop (and computationally efficient) optimal solution presented in [11], that minimizes

$$ J\left(\hat{\mathbf{R}}(t)\right) = \frac{1}{2}\sum_{i=1}^{2}\frac{1}{2}\left\|\hat{\mathbf{y}}_i^u(t) - \hat{\mathbf{R}}^T(t){}^{I}\mathbf{y}_i^u\right\|^2, $$

and that is omitted here due to the lack of space and as it can be found in [11]. The overall attitude estimation system is depicted in Fig. 1, where $\mathbf{K}(t)$ is the Kalman gain matrix. It is important to stress that the resulting structure is complementary: high bandwidth rate gyro measurements are combined with low bandwidth vector observations to determine a low frequency perturbation in the rate-gyro measurements and provide filtered estimates of the vector observations.

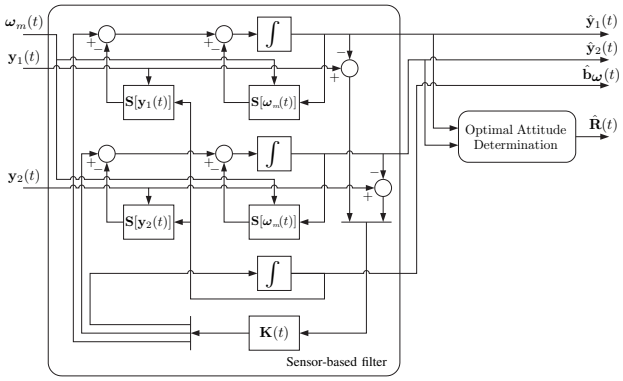

Fig. 1. Attitude Estimation System

Remark 3: There is nothing in the filter structure imposing any particular relation between $\hat{\mathbf{y}}_1(t)$ and $\hat{\mathbf{y}}_2(t)$. Therefore, it may happen, due to bad initialization of by accident, that $\hat{\mathbf{y}}_1(t)$ and $\hat{\mathbf{y}}_2(t)$ are parallel for some time t. In this case, the optimal solution presented in [11] is not well defined. On the other hand, the same happens if, for some time t, $\hat{\mathbf{y}}_1(t) = \mathbf{0}$ or $\hat{\mathbf{y}}_2(t) = \mathbf{0}$. If any of these situations was to happen, the sensor measurements could be used directly to obtain an estimate of the attitude. However, notice that the filter may be initialized with the first set of vector observations. In addition to that, it will be shown shortly that the filter convergence, which is global, is very fast, and warming-up delays below 1 s may be considered. Therefore, none of these situations are to happen in practice.

C. Single Vector Observations

When only one vector measurement is available, it is obviously impossible to determine the attitude. Nevertheless, some information is extracted. As an example, if the attitude is parameterized using the yaw, pitch, and roll Euler angles, the roll and pitch angles would be determined from gravitational field vector observations. Therefore, in this case, and in order to evaluate the performance of the proposed solution, two Euler angles are determined from the estimates provided by the Kalman filter, which is a reduced version of the filter proposed in Section IV-A. This is omitted due to the lack of space and as it is evident from the context.

D. Multiple Vector Observations

Although in the paper only up to two vector observations are considered, the proposed solution is trivially extended for multiple vector observations. Indeed, all that is required is to add more states to the system dynamics (14) and to modify the attitude determination algorithm to cope with more than two vector observations. This is quite useful as there is a myriad of commercially available sensors that provide vector measurements useful for attitude determination. As an example, there are nowadays star trackers that can track over 50 stars at a time. Notice that in this case the specificness of each sensor can still be directly incorporated in the filter design and colored noise is easily modeled, as opposed to tradition solutions that use the vector measurements solely to compute an instantaneous attitude measurement used to feed an observer or filter built on one of the many attitude representations.

V. Simulation Results

In order to evaluate the performance of the proposed filtering solutions, simulations were carried out using a fixed platform with unlimited rotation available on all axes, similar to, e.g., the calibration table 2103HT Series Multi-Axis Table, from Ideal Aerosmith. For performance evaluation purposes, and for the sake of illustrativeness, the rotation matrix was parameterized by yaw, pitch, and roll Euler angles, and oscillatory angular rates were applied, as given by

$$ \boldsymbol{\omega}(t) = \frac{\pi}{180}\begin{bmatrix} 2\sin\left(\frac{2\pi}{20}t\right) \\ 5\sin\left(\frac{2\pi}{30}t + \pi/2\right) \\ 0 \end{bmatrix} (rad/s)\,. $$

The evolution of the Euler angles is presented in Fig. 2. A

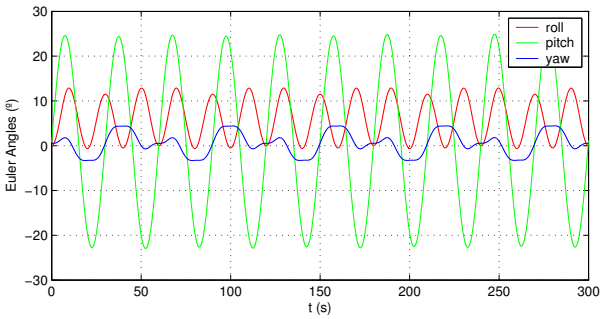

Fig. 2. Evolution of the Euler angles

low-cost, low-power IMU is considered, with three triads of orthogonally mounted rate gyros, accelerometers, and magnetometers. Two different cases are studied. In the first case, presented in Section V-A, the IMU is assumed to provide the magnetic and gravitational fields, as well as the angular velocity of the vehicle corrupted with a constant unknown bias. In the second case, discussed in Section V-B, loss of magnetic field measurements is addressed. Additive zero-mean white noise was considered for all sensors, with

standard deviation $0.015\,\mathrm{mG}$ and $0.05\,\mathrm{m/s^2}$ for the magnetometers and accelerometers, respectively, and $0.05\,^\circ/\mathrm{s}$ for the rate gyros, whose measurements were also corrupted by a constant bias equal to $\mathbf{b}_{\boldsymbol{\omega}} = [2\ -3\ 1]^T\ (^\circ)$. The sample rate was set to $100\,\mathrm{Hz}$ and numerical integration was carried out using a fourth-order Runge-Kutta method. Notice that there are low-cost IMU with better specifications, as well as better integration algorithms, but for the sake of clarity of performance evaluation, very low-cost specifications were considered.

A. Double vector observations

This section presents simulation results for double vector observations. The Kalman filter parameters were chosen according to the sensor noise levels,

$$\boldsymbol{\Xi} = \mathrm{diag}\left(0.015, 0.015, 0.015, 0.05, 0.05, 0.05, 10^{-6}, 10^{-6}, 10^{-6}\right),$$

$$\boldsymbol{\Theta} = \mathrm{diag}\left(0.015, 0.015, 0.015, 0.05, 0.05, 0.05\right),$$

and $\boldsymbol{\Psi} = \mathbf{0}$. No particular emphasis was given on the tuning process as the resulting performance with these simple parameters is very good. In practice, the spectral contents of the sensors noise may be experimentally approximated and frequency weights adjusted to improve the performance of the filter, see the examples provided in [14]. Moreover, correlation between the system disturbances $\mathbf{d}$ and the sensor noise $\mathbf{n}$ may also be considered. Since $\mathbf{x}_1$ and $\mathbf{x}_2$ are measured, these variables were initialized close to the true values. The initial bias estimate was set to zero.

The evolution of the filter error is depicted in Fig. 3 and, in greater detail, in Fig. 4. Notice that the convergence rate is very fast. Moreover, the gyro error noise level is well below the noise of the rate gyro measurements. The same happens, as expected, with the error level of the two vector estimates of the gravitational and magnetic field.

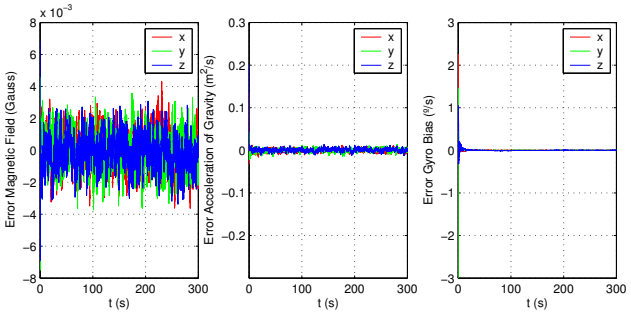

Fig. 3. Evolution of the filter error

In order to evaluate the overall attitude performance, the yaw, pitch, and roll Euler angles were computed from the estimated rotation matrix $\hat{\mathbf{R}}$. The evolution of the error of the Euler angles is depicted in Fig. 5, where the error is also shown for the Euler angles obtained directly from the sensor measurements, which is large due to the bad specifications of the sensors considered. The standard deviation of the steady-state error is shown in Table I, where the noise level of the Euler angles obtained directly from the vector measurements is also presented. The results evidence excellent performance and very fast convergence, in spite of the overall low-cost characteristics of the sensor suite.

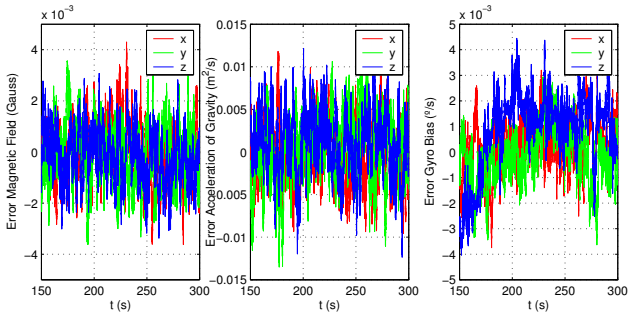

Fig. 4. Detailed evolution of the filter error

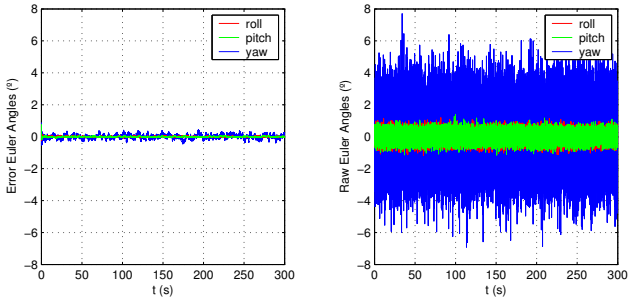

Fig. 5. Evolution of the error of the Euler angles

B. Single vector observations

The case of single vector observations is considered in this section. For that purpose, the previous simulation was modified and the magnetic field measurements discarded. Notice that this is quite possible from the practical point of view, as magnetic field anomalies are often. For attitude estimation purposes, other sensors may always be considered, but it is nevertheless interesting to see the achievable performance in terms of gyro bias estimation in the presence of single vector measurements. Furthermore, for dead-reckoning navigation systems such as Inertial Navigation Systems, the single possibility of gyro bias estimation greatly improves its performance degradation over time.

In addition to the loss of one vector observation, in this simulation the gyro bias is slowly time-varying, given by

$$\mathbf{b}_{\boldsymbol{\omega}}(t) = \frac{\pi}{180}\begin{bmatrix} 2 \\ -3 \\ 1 + \sin\left(\frac{2\pi}{600}t\right) \end{bmatrix}\ (rad/s).$$

Notice that slowly time-varying bias is a very common and undesirable characteristic of low-cost rate gyros. The filter parameters were chosen as

$$\boldsymbol{\Xi} = \mathrm{diag}\left(0.05, 0.05, 0.05, 10^{-2}, 10^{-2}, 10^{-2}\right),$$

$$\boldsymbol{\Theta} = \mathrm{diag}\left(0.05, 0.05, 0.05\right),$$

and $\boldsymbol{\Psi} = \mathbf{0}$. Again, no particular emphasis was given on the tuning process as the resulting performance with these simple parameters is very good.

The evolution of the filter error is depicted in Fig. 6 and, in greater detail, in Fig. 7. Notice that, as in the previous case, the convergence speed is very fast, and the error level remains confined to a very tight interval. In Fig. 8 the evolution of the gyro bias estimate is presented, along with the actual

TABLE I

STANDARD DEVIATION OF THE ERROR OF THE EULER ANGLES

Euler Angle	Proposed Solution	From vector measurements
roll (°)	0.0238	0.3062
pitch (°)	0.0204	0.2892
yaw (°)	0.1337	1.730

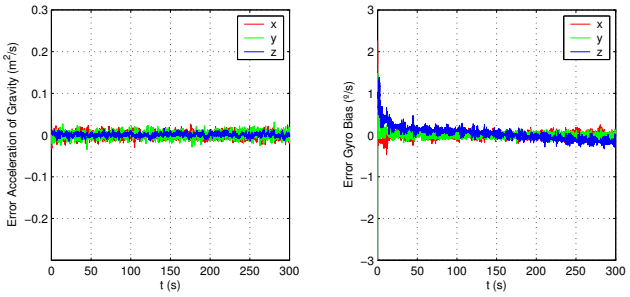

Fig. 6. Evolution of the filter error

values. This plot clearly evidences that the filter copes well with slowly time-varying gyro bias. Finally, the roll and pitch Euler angles are computed from the gravity vector estimate, and the evolution of the error depicted in Fig. 9, where the evolution of the error that results from computing these angles directly from the accelerometer measurements is also shown. The standard deviation is presented in Table II. It is interesting to see that there is a slight performance degradation, in comparison with the results presented in Section V-A, but the overall quality of the estimates is still very good, in spite of the presence of slowly time-varying bias and single vector observations.

TABLE II

STANDARD DEVIATION OF THE ERROR OF THE ROLL AND PITCH EULER ANGLES

Euler Angle	Proposed Solution	From vector measurements
roll (°)	0.0453	0.3054
pitch (°)	0.0430	0.2901

VI. CONCLUSIONS

This paper presented the analysis, design, and performance evaluation of sensor-based attitude estimation filters. Although the system dynamics for attitude estimation are inherently nonlinear, linear time-varying interpretations are possible after some quick algebraic manipulations. Taking

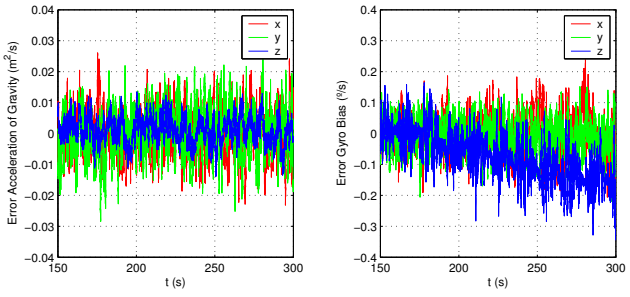

Fig. 7. Detailed evolution of the filter error

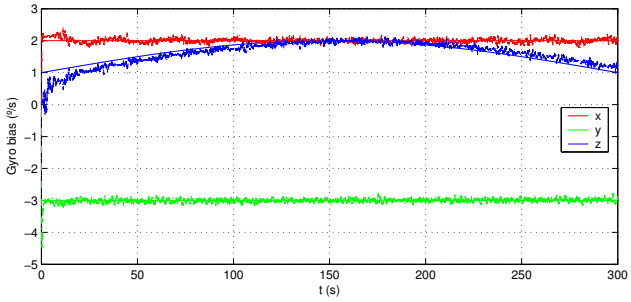

Fig. 8. Detailed evolution of the gyro bias (solid lines) and gyro bias estimate (dash

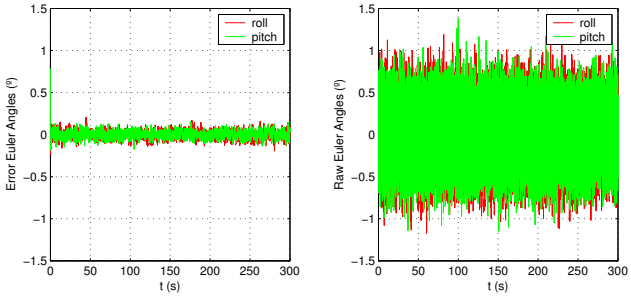

Fig. 9. Evolution of the error of the roll and pitch Euler angles

advantage of the new formulations, the observability properties of the systems were analyzed resorting to classic linear systems theory and globally asymptotically stable filters derived based on the well-known Kalman filter.

Classic attitude estimation solutions typically ignore the specificness of the sensors, which are basically used to construct instantaneous algebraic attitude measurements in one of many attitude representation, e.g., Euler angles, quaternions, rotation matrices, etc., and the filtering process takes place in one of these representations. In this paper the filtering process is carried out directly in the space of the measurements, allowing the specifications of each sensor, including frequency response characteristics, to be incorporated in the filter design process, which is therefore systematic. The proposed solutions are based on the kinematic model, which relies on angular velocity measurements provided by rate gyros to propagate the system state, and the gyro bias is also taken into account and explicitly estimated. The resulting structure is complementary, taking full advantage of the several sensor readings.

Two practical applications were presented. In the first case study, gravitational and magnetic field measurements are used, coupled with rate gyro readings, to estimate the attitude of a vehicle, as well as the rate gyro bias. In the second application loss of sensor information is addressed and only gravitational field measurements are considered together with the rate gyro readings corrupted by bias. In this last situation the goal is to estimate the rate gyro bias and restrict the attitude to a set of lower dimension, as it is evidently impossible to estimate the attitude with only one vector observation. Simulation results are included that illustrate the achievable performance in the presence of realistic measurements provided by low-cost, low-power sensor suites, and the solutions are also shown to cope well

with slowly time-varying gyro bias. Future work includes the implementation and experimental evaluation of the proposed solutions in several mobile platforms, including underwater and aerial vehicles, with different sets of sensors.

REFERENCES

[1] J. Crassidis, F. Markley, and Y. Cheng, "Survey of Nonlinear Attitude Estimation Methods," *Journal of Guidance, Control and Dynamics*, vol. 30, no. 1, pp. 12–28, Jan.-Feb. 2007.

[2] M. Shuster, "A Survey of Attitude Representations," *Journal of the Astronautical Sciences*, vol. 41, no. 4, pp. 439–517, Oct.-Dec. 1993.

[3] J. Farrell, "Attitude Determination by Kalman Filter," *Automatica*, vol. 6, no. 5, pp. 419–430, 1970.

[4] I. Bar-Itzhack and Y. Oshman, "Attitude Determination from Vector Observations: Quaternion Estimation," *IEEE Trans. on Aerospace and Electronic Systems*, vol. 321, no. 1, pp. 128–136, 1985.

[5] J. Thienel and R. Sanner, "A Coupled Nonlinear Spacecraft Attitude Controller and Observer With an Unknown Constant Gyro Bias and Gyro Noise," *IEEE Trans. on Automatic Control*, vol. 48, no. 11, pp. 2011–2015, Nov. 2003.

[6] H. Rehbinder and B. Ghosh, "Pose Estimation Using Line-Based Dynamic Vision and Inertial Sensors," *IEEE Trans. on Automatic Control*, vol. 48, no. 2, pp. 186–199, Feb. 2003.

[7] R. Mahony, T. Hamel, and J.-M. Pflimlin, "Nonlinear Complementary Filters on the Special Orthogonal Group," *IEEE Trans. on Automatic Control*, vol. 53, no. 5, pp. 1203–1218, June 2008.

[8] J. Vasconcelos, R. Cunha, C. Silvestre, and P. Oliveira, "Landmark Based Nonlinear Observer for Rigid Body Attitude and Position Estimation," in *Proc. 46th IEEE Conf. on Decision and Control*, New Orleans, LA, USA, Dec. 2007, pp. 1033–1038.

[9] G. Wahba, "A Least Squares Estimate of Spacecraft Attitude," *SIAM Review*, vol. 7, no. 3, p. 409, July 1965.

[10] M. Shuster and S. Oh, "Three-Axis Attitude Determination from Vector Observations," *Journal of Guidance, Control and Dynamics*, vol. 4, no. 1, pp. 70–77, Jan.-Feb. 1981.

[11] F. Markley, "Optimal Attitude Matrix from Two Vector Measurements," *Journal of Guidance, Control and Dynamics*, vol. 31, no. 3, pp. 765–768, May-June 2008.

[12] M. Bryson and S. Sukkarieh, "Vehicle Model Aided Inertial Navigation for a UAV using Low-Cost Sensors," in *Proc. Australasian Conference on Robotics and Automation*, Canberra, Australia, Dec. 2004.

[13] R. W. Brockett, *Finite Dimensional Linear Systems*. Wiley, 1970.

[14] P. Batista, C. Silvestre, and P. Oliveira, "Position and Velocity Navigation Filters for Marine Vehicles," in *Proc. 17th IFAC World Congress*, Seoul, Korea, July 2008.

[15] R. Kalman and R. Bucy, "New Results in Linear Filtering and Prediction Theory," *Journal of Basic Eng., Trans. ASME, Series D*, vol. 83, no. 3, pp. 95–108, Mar. 1961.

[16] B. D. O. Anderson, "Stability properties of Kalman-Bucy filters," *Journal of Franklin Institute*, vol. 291, no. 2, pp. 137–144, Feb. 1971.

APPENDIX I
PROOF OF LEMMA 1

Firstly, notice that the case $C = 0$ is trivial. Indeed, if $C = 0$, then

$$\underset{t \in \mathcal{I}}{\forall} \quad : \quad \dot{\mathbf{f}}(t) = \dot{\mathbf{f}}(t^*)$$

and therefore

$$\begin{aligned} \mathbf{f}(t_0 + \delta) &= \dot{\mathbf{f}}(t^*) \int_{t_0}^{t_0+\delta} \int_{t_0}^{\sigma_1} \dots \int_{t_0}^{\sigma_{i-1}} d\sigma_i \dots d\sigma_1 \\ &= \frac{\delta^i}{i!} \dot{\mathbf{f}}(t^*), \end{aligned}$$

which implies (8). The remainder of the proof considers $C > 0$. Suppose that (6) and (7) are true. Then, using simple norm inequalities, it is possible to write

$$\left\| \dot{\mathbf{f}}(t^*) \right\|_\infty \geq \frac{1}{\sqrt{n}} \alpha^*$$

and

$$\max_{t \in \mathcal{I}} \left\| \ddot{\mathbf{f}}(t) \right\|_\infty \leq C.$$

Let

$$k := \arg \max_{j=1,\dots,n} \left| \dot{f}_j(t^*) \right|,$$

where

$$\dot{\mathbf{f}}(t) = \begin{bmatrix} \dot{f}_1(t) \\ \vdots \\ \dot{f}_n(t) \end{bmatrix}.$$

Evidently,

$$\left| \dot{f}_k(t^*) \right| \geq \frac{1}{\sqrt{n}} \alpha^*$$

and

$$\max_{t \in \mathcal{I}} \left| \ddot{f}_k(t) \right| \leq C. \tag{15}$$

Resorting to the Lagrange's Theorem, it is possible to write that

$$\left| \dot{f}_k(t) - \dot{f}_k(t^*) \right| = \left| \ddot{f}_k(\xi(t))(t - t^*) \right| \tag{16}$$

for all $t \in \mathcal{I}$, where $\xi(t) \in]t_0, t_f[$. Using simple norm inequalities and (15) in (16) gives

$$\left| \dot{f}_k(t) - \dot{f}_k(t^*) \right| \leq C |t - t^*|.$$

and therefore

$$\dot{f}_k(t) \geq \dot{f}_k(t^*) - C |t - t^*|$$

for all $t \in \mathcal{I}$. Now assume, without loss of generality, that $\dot{f}_k(t^*) > 0$. Then, there exists an interval $\mathcal{I}_1 = [t_1, t_2] \subset \mathcal{I}$, $t_1 < t_2$, where either $t_1 = t^*$ or $t_2 = t^*$, and with length

$$T_1 := \frac{1}{2} \min \left(T, \frac{\alpha^*}{C} \right),$$

such that

$$\underset{t \in \mathcal{I}_1}{\forall} \quad : \quad \dot{f}_k(t) \geq \dot{f}_k(t^*) - C |t - t^*| > 0. \tag{17}$$

Integrating (17) on $\mathcal{I}_1$ gives

$$\int_{\mathcal{I}_1} \dot{f}_k(t)\, dt \geq \beta > 0,$$

where

$$\beta := T_1 \left(\alpha^* - \frac{C T_1}{2} \right) > 0.$$

Now, notice that

$$\begin{aligned} f_k(t_2) &= \int_{t_0}^{t_2} \dot{f}_k(t)\, dt \\ &= \int_{t_0}^{t_1} \dot{f}_k(t)\, dt + \int_{\mathcal{I}_1} \dot{f}_k(t)\, dt. \end{aligned}$$

If

$$f_k(t_2) \neq 0$$

then

$$\underset{\substack{0 < \delta_1^* \leq T \\ \beta^* > 0}}{\exists} \quad : \quad |f_k(t_0 + \delta_1^*)| \geq \beta_1^*.$$

Otherwise, it must be

$$f_k\left(t_0+t_1\right)=-\int_{\mathcal{I}_1}\dot{f}_k\left(t\right)dt\neq 0,$$

which implies that

$$\begin{array}{c}\exists\\ 0<\delta_2^*<T\\ \beta_2^*>0\end{array}\quad:\quad\left|f_k\left(t_0+\delta_2^*\right)\right|\geq\beta_2^*.$$

Either way,

$$\begin{array}{c}\exists\\ 0<\delta^*\leq T\\ \beta^*>0\end{array}\quad:\quad\left|f_k\left(t_0+\delta^*\right)\right|\geq\beta^*$$

and, using simple norm inequalities

$$\begin{array}{c}\exists\\ 0<\delta^*<T\\ \beta^*>0\end{array}\quad:\quad\left\|\mathbf{f}\left(t_0+\delta^*\right)\right\|\geq\beta^*,$$

which concludes the proof.